Review of the Aerosol Mass Tracking Method in the ISFRA Fission Product Transport Module for SFR Accident Analyses

Churl Yoon* and Seok Hun Kang
Korea Atomic Energy Research Institute, 111 Daedeok-daero 989 Beon-gil, Yuseong-gu, Daejeon 34057, Korea
**Corresponding author: cyoon@kaeri.re.kr*

1. Introduction

A pool-type sodium-cooled fast reactor has been selected and developed as the prototype Gen-IV sodium-cooled fast reactor (PGSFR) at KAERI since 1987. Main advantage of the PGSFR is to reduce the radioactive nuclear waste amount from operating nuclear power reactors by transmutation. Other advantages of the PGSFR are the high safety level in the design and the efficient electric power generation.

In the safety analysis of the PGSFR, it is essential to predict the behavior of the radioactive fission product (FP) released from the core and estimate exactly the released amount to the environment under postulated nuclear power plant accidents. Under the contract with the KAERI, the Fauske & Associates, LLC (FAI) had developed the ISFRA (Integrated Sodium Fast Reactor Analysis) computer software by 2016. The ISFRA computer software is a best estimate computing tool used to simulate the consequences of beyond design basis accident transients and postulated severe accidents in the PGSFR. This computer program was designed to be a fast running simulation software used to accurately predict the initial transient and the subsequent release and transport of fission products.[1]

Even though it is one of the main concerns in event consequence evaluation to predict the aerosol FP behavior inside the containment and the FP release rate to the environment in a certain detail level, the ISFRA aerosol analysis models predict only the total masses of suspended and deposited aerosols without any information of detailed particle size distribution and particle material composition. Therefore, the ISFRA aerosol models are under improvement to meet the regulatory requirements, which could be achieved through modifying the existing correlations of the FAI aerosol models or adopting an advanced method such as the Moment method or the MAEROS method. The purposes of this study are to review and understand the aerosol mass tracking method of the ISFRA FP transport analysis module, considering the aerosol model improvement by modifying the existing FAI aerosol correlations.

2. ISFRA Aerosol Mass Tracking Method

The kinetic equation of simultaneous coagulating and depositing particles being continuously supplied with particles and having a continuous particle size distribution is as follows:

$$\frac{\partial n(v,t)}{\partial t} = \frac{1}{2}\int_0^v K(\bar{v}, v-\bar{v}) n(\bar{v},t) n(v-\bar{v},t)\, d\bar{v} - \int_0^\infty K(\bar{v},v) n(\bar{v},t) n(v,t)\, d\bar{v} - \frac{n(v,t)u(v)}{h} + \dot{n}_p(v) \quad (1)$$

The functional form for the collision kernel $K(v, \tilde{v})$ that appears in Eq. (1) depends on the coagulation mechanisms being assumed to govern the behavior of the aerosol. The mechanisms causing relative motion between particles, and thus coagulation, and accounted for here, are Brownian motion of the particles and gravitational settling. Then the collision kernel can be expressed as follows:

$$K(v,\bar{v}) = K_B(v,\bar{v}) + K_g(v,\bar{v}) \quad (2)$$

For particles larger than the gas mean free path, the collision kernels for the Brownian and gravitational coagulation mechanisms, written in terms of particle volume, are

$$K_B(v,\bar{v}) = \frac{\gamma K_0}{2\chi}\left(v^{1/3}+\bar{v}^{1/3}\right)\left(v^{-1/3}+\bar{v}^{-1/3}\right) \quad (3)$$

$$K_g(v,\bar{v}) = \frac{2\pi g \rho \gamma^2}{9\mu\alpha^{1/3}\chi}\cdot\varepsilon(v,\bar{v})\cdot\left(\frac{3}{4\pi}\right)^{4/3} \cdot\left(v^{1/3}+\bar{v}^{1/3}\right)^3\left|\bar{v}^{1/3}-v^{1/3}\right| \quad (4)$$

Here, $\varepsilon(v,\bar{v})$ is in the following functional form.[2]

$$\varepsilon(v,\bar{v}) = \frac{3}{2}\left(\frac{v^{1/3}}{v^{1/3}+\bar{v}^{1/3}}\right)^2 \quad (5)$$

Finally, the settling velocity for the small particles of interest in aerosol transport is accurately represented by Stokes' law.

$$u(v) = \frac{2}{9}\left(\frac{3}{4\pi}\right)^{2/3}\cdot\frac{\alpha^{1/3} g \rho v^{2/3}}{\chi\mu} \quad (6)$$

Taking the first moment of Eq. (1) to temporarily avoid the many complications, the total aerosol mass concentration is expressed as

Table I: Primary dimensions for dimensional analysis [4]

Primary dimension	SI unit	BG unit	Conversion factor
Mass {M}	Kilogram (kg)	Slug	1 slung = 14.5939 kg
Length {L}	Meter (m)	Foot (ft)	1 ft = 0.3048 m
Time {T}	Second (s)	Second (s)	1 s = 1 s
Temperature {Θ}	Kelvin (K)	Rankine (^{o}R)	1 K = 1.8 ^{o}R

$$m(t)=\rho\int_0^\infty vn(v,t)dv \cdot \quad (7)$$

Then, Eq. (1) becomes the ordinary differential equation:

$$\frac{dm(t)}{dt}=-\lambda(t)m(t)+\dot{m}_p \quad (8)$$

Here, $\dot{m}_p(t)=\rho\int_0^\infty v\dot{n}_p(v,t)dv$ (9)

$$\lambda(t)=\frac{\int_0^\infty vn(v,t)u(v)dv}{h\int_0^\infty vn(v,t)dv} \quad (10)$$

2.1 Aerosol Similitude and Dimensional Analysis

In the consequence analyses of postulated nuclear power plant accidents, it is essential for understanding the physical phenomena to evaluate the total suspended mass and the particle size distribution of aerosols undergoing Brownian coagulation and gravitational settling. Previous works with Eq. (1) have shown that as time increases the particle size distribution becomes independent of the initial distribution of sizes. It has been also shown theoretically that particle size spectra in systems coagulating by Brownian motion reach a constant "self-preserving form" (with respect to particle size) independent of the initial distribution after a sufficiently long time.[3] We shall refer here to the tendency for aerosol distributions to approach the same form as the condition of "aerosol similitude." To be similar it is evidently necessary that the aerosol particle size distributions can be made identical by selecting suitable scale factors for the particle number density, the particle volume, and time.

For the dimensional analysis of the governing equation, the 'principle of dimensional homogeneity' should be stated as follows [4]:

> If an equation truly expresses a proper relationship between variables in a physical process, it will be dimensionally homogeneous; i.e., each of its additive terms will have the same dimensions.

Table 1 summaries some primary dimensions and their units. With these primary dimensions, secondary dimensions such as velocity and acceleration have dimensions of $\{LT^{-1}\}$ and $\{LT^{-2}\}$, respectively:

$\{V\}=\{LT^{-1}\}$ and $\{g\}=\{LT^{-2}\}$.

2.2 Similarity of Aging Aerosols

To avoid the complexity of the above governing equations, FAI transformed the aerosol equations to dimensionless forms which will readily reveal the nature of the similarities which exist among seemingly different aerosols. This 'similarity' means that as time increases the particle size distribution becomes independent of the initial distribution of sizes. For aging aerosols, $\dot{n}_p(v)=0$. The governing equations are reduced to universal form, by introducing the dimensionless variables as follows:

$n(v,t)=c_1N(\upsilon,\tau)$, $v=c_2\upsilon$, and $t=c_3\tau$.

By solving the governing equations for c_1, c_2, and c_3, quantities of m(t), λ(t), and $\dot{m}_p$ can be transformed into the dimensionless parameters of M(τ), Λ(τ), and $\dot{M}_p$.

Substituting these dimensionless variables into the variables of n(v,t), v, and t, Eq. (1) becomes

$$\frac{\partial c_1N(\upsilon,\tau)}{\partial(c_3\tau)}=\frac{1}{2}\int_0^{c_2\upsilon}K(\bar{v},v-\bar{v})\cdot c_1N(\bar{v},\tau)\cdot c_1N(\upsilon-\bar{v},\tau)\cdot d(c_2\bar{v})-\int_0^\infty K(\bar{v},v)\cdot c_1N(\bar{v},\tau)\cdot c_1N(\upsilon,\tau)\cdot d(c_2\bar{v})-\frac{c_1N(\upsilon,\tau)u(v)}{h} \quad (11)$$

Eliminating the dimensionless variables and substituting Eq. (2) into Eq. (11), dimensional analysis gives the following equation:

$$\left\{\frac{c_1}{c_3}\right\}=\left\{\frac{{c_1}^2c_2}{2}\int_0^{c_2\upsilon}K_B(v,v-\bar{v})\cdot N(\bar{v},\tau)\cdot N(\upsilon-\bar{v},\tau)\cdot d\bar{v}\right\}+\left\{\frac{{c_1}^2c_2}{2}\int_0^{c_2\upsilon}K_g(v,v-\bar{v})\cdot N(\bar{v},\tau)\cdot N(\upsilon-\bar{v},\tau)\cdot d\bar{v}\right\}-\left\{{c_1}^2c_2\int_0^\infty K_B(v,\bar{v})\cdot N(\bar{v},\tau)\cdot N(\upsilon,\tau)\cdot d\bar{v}\right\}-\left\{{c_1}^2c_2\int_0^\infty K_g(v,\bar{v})\cdot N(\bar{v},\tau)\cdot N(\upsilon,\tau)\cdot d\bar{v}\right\}-\left\{\frac{c_1N(\upsilon,\tau)u(v)}{h}\right\} \quad (12)$$

Substituting K_B and K_g with Eqs. (3) and (4), the dimensional analysis of the first and the third terms of RHS gives

$$c_1c_2c_3=\frac{\chi}{\gamma K_0} \quad (13)$$

For the dimensional homogeneity of the second and the fourth terms of RHS,

$$c_1{c_2}^{7/3}c_3=\frac{\mu\alpha^{1/3}\chi}{g\rho\gamma^2} \quad (14)$$

From the dimensional analysis of the last term of RHS,

$$c_2^{2/3}c_3=\frac{h\chi\mu}{\alpha^{1/3}g\rho} \quad (15)$$

One can obtain the unknowns of c_1, c_2, and c_3 by solving the system of Eqs. (13) ~ (15) as follows:

$$c_1=\left(\frac{\alpha g^5\rho^5}{\gamma^3{K_0}^5\mu^5h^4}\right)^{1/4};\ c_2=\left(\frac{\alpha^{1/3}\mu K_0}{\gamma g\rho}\right)^{3/4};\ c_3=\left(\frac{\chi^2\gamma\mu h^2}{\alpha g\rho K_0}\right)^{1/2}.$$

On the other hand, the dimensionless total suspended aerosol mass M is transformed from $m(t)$ as follows:

$$M(\tau)=\int_0^\infty \upsilon N(\upsilon,\tau)d\upsilon=\left(\frac{\gamma^9gh^4}{\alpha^3K_0\mu\rho^3}\right)^{1/4}\cdot m(t) \quad (16)$$

The dimensionless decay constant is defined and expressed as the below.

Table 2: Scaling coefficients for macroscopic aerosol properties

Time, τ	Particle volume, υ	Particle number density, *N*
$\left(\frac{\alpha g\rho K_0}{\chi^2\gamma\mu h^2}\right)^{1/2}\cdot t$	$\left(\frac{\gamma g\rho}{\alpha^{1/3}\mu K_0}\right)^{\frac{3}{4}}\cdot v$	$\left(\frac{\gamma^3 K_0{}^5\mu^5 h^4}{\alpha g^5\rho^5}\right)^{1/4}\cdot n$
Mass density, *M*	Decay constant, *Λ*	Particle production rate, $\dot{N}_p$
$\left(\frac{\gamma^9 g h^4}{\alpha^3 K_0\mu\rho^3}\right)^{\frac{1}{4}}\cdot m$	$\left(\frac{\gamma\chi^2\mu h^2}{\alpha K_0 g\rho}\right)^{1/2}\cdot\lambda$	$\left(\frac{\gamma^5\chi^4 K_0{}^3\mu^7 h^8}{\alpha^3 g^7\rho^7}\right)^{\frac{1}{4}}\cdot\dot{n}_p$

$$\Lambda(t)=\frac{\int_0^\infty \upsilon^{(1+2/3)}N(\upsilon,\tau)d\upsilon}{\int_0^\infty \upsilon N(\upsilon,\tau)d\upsilon}=\left(\frac{\gamma\chi^2\mu h^2}{\alpha K_0 g\rho}\right)\cdot\lambda \qquad (17)$$

2.3 Similarity of Steady-State Aerosols

The particle size distribution of an aerosol continually reinforced by the introduction of particles at a steady rate and losing particles by sedimentation will ultimately achieve an equilibrium condition in which $\partial n(v,t)/\partial t=0$. Here, time does not enter into the coagulation equation but of course the source term $\dot{n}_p(v)$ must be retained. It can readily be shown by the method of the preceding section that the scalings for the quantities *n*, *v*, and *m* of an aerosol in steady state are given as in the previous section. Similar transformations can be derived by introducing the dimensionless parameters υ, τ, *N*(υ,τ), and an additional dimensionless particle source rate $\dot{N}_p(\upsilon)$ as follows:

$n(v,t)=d_1N(\upsilon,\tau)$, $v=d_2\upsilon$, $t=d_3\tau$ and

$\dot{n}_p(\upsilon)=d_4\dot{N}_p(\upsilon)$.

By the dimensional analyses with the above equations into Eq. (1) with $\partial n(v,t)/\partial t=0$, one can obtain algebraic compatibility equations for the coefficients d_1, d_2, d_3, and d_4 as previous. Solving these algebraic equations, we obtain the transformations as follows:

$d_1=c_1$, $d_2=c_2$, and $d_3=c_3$.

From the dimensional analysis of the last term of RHS,

$$d_4=\frac{d_1}{d_3}=\left(\frac{\alpha g^5\rho^5}{\gamma^3 K_0{}^5\mu^5 h^4}\right)^{1/4}\left(\frac{\alpha^2 g^2\rho^2 K_0{}^2}{\chi^4\gamma^2\mu^2 h^4}\right)^{1/4}=\left(\frac{\alpha^3 g^7\rho^7}{\gamma^5\chi^4 K_0{}^3\mu^7 h^8}\right)^{1/4}$$

Therefore, the dimensionless particle production rate is

$$\dot{N}_p(v)=\left(\frac{\gamma^5\chi^4 K_0{}^3\mu^7 h^8}{\alpha^3 g^7\rho^7}\right)^{1/4}\cdot\dot{n}_p(v) \qquad (18)$$

A physically more significant parameter is the dimensionless total mass introduction rate of particles $\dot{M}_p$, which can be related directly to $\dot{N}_p(v)$ by Eq. (9)

$$\dot{M}_p=\left(\frac{\gamma^{11}\chi^4\mu h^8}{\alpha^5 g K_0^3\rho^5}\right)^{1/4}\cdot\dot{m}_p=\int_0^\infty v\dot{N}_p(v)dv \qquad (19)$$

The obtained dimensionless variables for aging (decaying) and steady-state aerosols are summarized in Table 2.

3. ISFRA Aerosol Mass Reduction Correlations

The scaling factors in Table 2 do not include any of the properties of the initial distribution. Thus the condition of aerosol similarity is achieved with these scale factors only after sufficient coagulation takes place or, equivalently, time elapses so that the individual peculiarities related to the initial distribution of a particular aerosol are forgotten.

The results of numerical calculations for the evolution of the sectionalized particle mass distributions at dimensionless aging times τ = 1.0 and 2.0 for two different aerosols losing mass by sedimentation are shown in Fig. 1. MAEROS [5] numerical technique was used for the calculations, which is based upon diving the particle size domain into sections and dealing with one integral quantity in each section. In the figure, the aerosols with different initial size distributions and properties have the similar dimensionless particle size spectrums after a dimensionless time. Therefore, it is clearly shown in Fig. 1 that the similarity principle is approached after sufficient time has passed.

To determine the functional relationships of *Λ*(*M*), FAI obtained empirical fitting equations based on many exact numerical solutions and experimental studies. Figure 2 shows the dimensionless removal rate constant as a function of dimensionless suspended aerosol mass concentration, from the measured aerosol mass concentrations and removal rates of the ABCOVE experiments. The lower dashed curve corresponds to aerosols continually supplied with particles, under

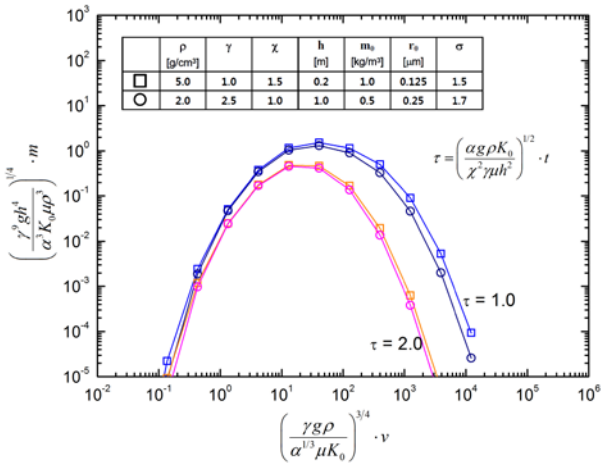

Fig. 1. Particle mass distribution at dimensionless aging times t = 1.0 and 2.0 of two different aerosols losing mass by sedimentation and undergoing Brownian and gravitational coagulation. (Reproduction of Figure 1 in [6])

steady-state conditions. The upper dotted curve is the dimensionless removal rate versus dimensionless mass relation for decaying aerosols in the absence of a source. The obtained algebraic fit equations for the curves are:

$$\Lambda_{SED}^{SS} = 0.266M^{0.282}\left(1+0.189M^{0.8}\right)^{0.695} \quad (20)$$

$$\Lambda_{SED}^{D} = 0.528M^{0.235}\left(1+0.473M^{0.754}\right)^{0.786} \quad (21)$$

Written in dimensionless form, steady-state and decaying conditions are expressed as follows:

$$\frac{dM}{d\tau} = -\Lambda_{SED}^{SS}(M)\cdot M + \dot{M}_p = 0 \quad (22)$$

$$\frac{dM}{d\tau} = -\Lambda_{SED}^{D}(M)\cdot M \quad (23)$$

4. Conclusions

In this research, the dimensionless scaling factors and the correlations in the aerosol mass tracking method of the ISFRA FP transport analysis module were reviewed by following the derivation procedure. The knowledge obtained in this study will be used as a basis for the improvement of the ISFRA aerosol models in the future researches.

ACKNOWLEDGMENTS

This work was supported by the National Research Foundation of Korea (NRF) grant funded by the Korea government (Ministry of Science and ICT) (No. NRF-2012M2A8A2025624)

NOMENCLATURE

h	effective height for aerosol deposition [m]
k	Boltzmann constant
$K(v, \tilde{v})$	kernel representing the frequency of binary collisions between particles of volume v and $\tilde{v}$
K_0	normalized Brownian collision coefficient (= $4kT/(3\mu)$)
m	total mass concentration of the suspended aerosols [kg/m^3]
$\dot{m}_p$	aerosol mass production rate [kg/m^3/s]
M	dimensionless total suspended aerosol mass
$\dot{M}_p$	dimensionless source rate
n	particle size distribution function [m^{-3}]
$\dot{n}_p$	source rate of particles [m^{-3}s^{-1}]
$N(\upsilon,\tau)$	dimensionless particle distribution function
v	particle volume [m^3]
t	time [s]
T	carrier gas temperature [K]
u	particle deposition or removal velocity [m/s]
α	density correction factor [-]
χ	particle settling shape factor [-]
$\varepsilon(v,\bar{v})$	capture coefficient [-]
γ	collision shape factor [-]

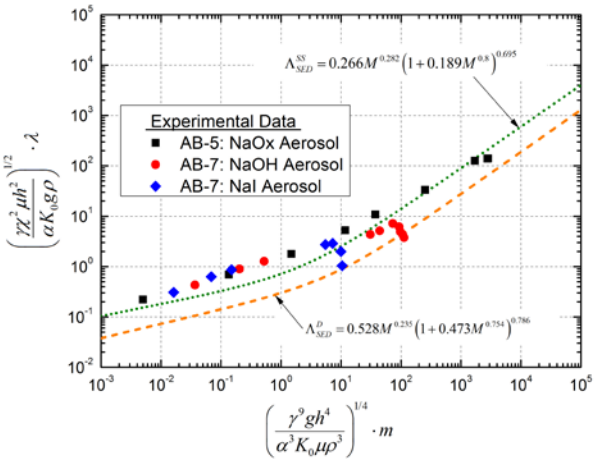

Fig. 2. Dimensionless aerosol removal rate constant for sedimentation as a function of dimensionless suspended mass concentration; steady-state and aging aerosol curves and experimental data. (Reproduction of Figure 1 in [7])

λ	aerosol removal rate constant [s^{-1}]
Λ	dimensionless decay constant
μ	viscosity of the carrier gas [kg/m/s]
ρ	density of the aerosol material [kg/m^3]
τ	dimensionless time
υ	dimensionless particle volume

Superscripts

D	decaying aerosol
SS	steady-state

Subscripts

B	Brownian (coagulation)
g	gravitational (coagulation)
SED	sedimentation

REFERENCES

[1] Fauske & Associates, LLC, *ISFRA user manual*. FAI Report, FAI/16-1089, p. 10, 2016.
[2] N. A. Fuchs, *The Mechanics of Aerosols*, Pergamon, Oxford, 1964.
[3] Fauske & Associates, LLC, "Technical Support for Issue Resolution", FAI/85-27, July 1985.
[4] F. M. White, *Fluid Mechanics*, 3rd Ed., McGraw-Hill, Inc., NJ, USA, 1994.
[5] F. Gelbard, *The MAEROS user Manual*, NUREG/CR-1391, SAND80-0822, 1982.
[6] M. Epstein and P. G. Ellison, "A Principle of Similarity for Describing Aerosol Particle Size Distribution", Journal of Colloid & Interface Science, Vol. 119, No. 1, 1987.
[7] M. Epstein and P. G. Ellison, "Correlations of the Rate of Removal of Coagulating and Depositing Aerosols for Application to Nuclear Reactor Safety Problems", Nuclear Engineering and Design, Vol. 107, pp. 327-344, 1988.
[8] E. H. Ryu, et al., "Correlation Confirmation on Removal Rate for Coagulating and Depositing Aerosols", KNS Spring Meeting, Jeju, 2017.